GEOMETRY OF AUTOMATICALLY CONTROLLED VEHICLE GUIDEWAYS FOR COMFORT

M. Balachandra and J. L. Dais, University of Minnesota

An analytical method is proposed for the design of guideway elements subject to jerk and acceleration limits. The method generalizes the limits on lateral jerk and acceleration familiar in highway design to the fore-aft and vertical modes. It is proposed that, under combinations of these modes, the magnitudes of the jerk and effective acceleration vectors must be limited. Equations describing the level of discomfort are derived for both constant and variable-speed motion along horizontal and vertical curves. The equations explicitly include the effect of superelevation. A four-spiral switch for use in a personalized rapid transit system is analyzed in detail. It is found that a length reduction of more than 25 percent is possible by using superelevation. A right angle turn composed of two spirals and a circular arc is detailed. It is found that the use of superelevation can reduce the magnitudes of the effective jerk and acceleration vectors by more than 50 percent. Finally, a four-spiral grade change is detailed. Discomfort is investigated and compared for constant speed and zero fore-aft thrust motion. It is shown that the usual analytical approach that includes only the centripetal component of acceleration and jerk can lead to considerable error in predicting discomfort.

•IT IS well known that human beings experience discomfort when subjected to acceleration and jerk. Considerable experimental work has been done to evaluate the effects of particular types of acceleration and jerk and the data have been used in the geometric design of automotive test tracks (1, 2), highways (3), and railroads (4). Physiological mechanisms associated with acceleration discomfort have also been extensively studied (5). Most of the work has been concerned with accelerations and jerks in one mode: lateral, fore-aft, or vertical. There has been very little work describing discomfort levels due to combinations of these modes, although the importance of such work has been noted (5, 6), and the authors are aware of one experimental study on the subject (7).

Evaluation of discomfort in combined modes has not been important for the geometric design of highways and railroads. Only the lateral comfort limits are used for the geometric design of highways and railroads. Curvatures in the vertical plane are limited by visibility requirements and grades by engine power and surface friction limitations. In recent days, however, there has been considerable interest in automatically controlled vehicle systems like personalized rapid transit (PRT) and dual mode transit. In such systems, vehicles run on fixed guideways with off-line stations (6, 8, 9).

Because of electronic sensing, novel types of vehicle suspension (e.g., air or magnetic), and a uniform power-weight ratio, the highway limitations on grade and vertical curvatures would not apply. Thus, the geometric design of guideway elements for these networks will to a large degree be determined by comfort criteria. Furthermore, in networks with closely spaced stations and interchanges, space limitations would be very stringent. Such limitations require that geometric design incorporate quantitative criteria involving combinations of fore-aft, lateral, and vertical accelerations and jerks.

In this paper a mixed mode measure of discomfort is developed by defining an "effective" acceleration vector $\underline{a}_e$ as shown in Figure 1. $\underline{a}_e$ is the difference between the total acceleration (including gravity) and the acceleration associated with self weight, $-g\underline{n}$. In three dimensions, the fore-aft component of acceleration, if present, would be

vectorially included in $\underset{\sim}{a}_e$. The magnitude of $\underset{\sim}{a}_e$ is termed the acceleration discomfort index and is assumed to be a direct quantitative measure of the amount of acceleration discomfort. $\underset{\sim}{J}_e$, the time derivative of $\underset{\sim}{a}_e$ in a frame of reference attached to the vehicle, is termed the effective jerk vector. The magnitude of $\underset{\sim}{J}_e$ is assumed to measure the amount of jerk discomfort. From these assumptions, it is possible to derive expressions for the amount of jerk and acceleration discomfort in terms of the vehicle speed, speed change, and guideway centerline geometry and superelevation.

Three examples of geometric design of components of a PRT network are presented as applications of the methods of the paper. The techniques described are also applicable to the geometric design of other transportation systems. The first example is concerned with a four-spiral switch that connects an off-line acceleration or deceleration lane with the main line. Dais used the four-spiral combination horizontally as an unbanked switch for PRT networks (12). In this paper we investigate the possibility of decreasing the length of such a switch by banking the guideway.

A right angle turn using a circular arc with spiral easement at both ends is described next. The discomfort along such a curve and the effect of superelevation are investigated for constant speed motion along the curve.

The use of spiral curves along with a straight inclined line to achieve a grade change makes up the third example of the paper. Motion along such a curve is considered both with zero fore-aft thrust and with constant speed, and it is shown that the two differ significantly in terms of the discomfort caused. The work generalizes previous work (1) by using formulas that include the fore-aft components as well as the normal modes. The error introduced by considering only the centripetal component of acceleration (1) is also investigated.

THEORETICAL DEVELOPMENT

Consider a subject in a moving vehicle in some preferred configuration like sitting or lying down. The basic principle postulated here is that, in the presence of accelerations in addition to that of gravity, the discomfort experienced by the subject is a function of the vectorial difference between the total body force on the subject and a datum corresponding to his self weight. Although this idea has been stated by others (1, 5), its mathematical consequences in connection with transportation guideway design have not been fully explored.

To make the above concept more explicit, consider a triad of mutually perpendicular unit vectors fixed in the vehicle with $\underset{\sim}{t}$ tangent to the guideway centerline in the direction of travel of the vehicle, $\underset{\sim}{n}$ normal to the vehicle, and $\underset{\sim}{\ell}$ in the lateral direction of the vehicle. n and $\underset{\sim}{\ell}$ are shown in Figure 1. Then we define the effective acceleration vector by

$$\underset{\sim}{a}_e = -g\underset{\sim}{n} - \underset{\sim}{g} + \underset{\sim}{a} \tag{1}$$

where

$\underset{\sim}{a}$ = acceleration of the vehicle and
$\underset{\sim}{g}$ = acceleration of gravity.

It is assumed that $|\underset{\sim}{a}_e|$ determines the level of acceleration discomfort. In equation form,

$$\phi = |\underset{\sim}{a}_e| = (\underset{\sim}{a}_e \cdot \underset{\sim}{a}_e)^{1/2} \tag{2}$$

where ϕ is termed the acceleration discomfort index. Analogously, it is postulated that jerk discomfort is essentially due to the subject's having to adjust to a changing force field and consequently may be analyzed by considering an effective jerk vector $\underset{\sim}{J}_e$ defined by

$$\underset{\sim}{J}_e = \frac{d\underset{\sim}{a}_e}{dt} \tag{3}$$

In Eq. 3 the differentiation is assumed to be performed in the $\underset{\sim}{n}$, $\underset{\sim}{\ell}$, and $\underset{\sim}{f}$ frames of reference. The level of discomfort due to jerk is expressed by means of a jerk discomfort index ψ. This index is assumed to be given by the magnitude of the effective jerk vector. In equation form,

$$\psi = |\underset{\sim}{J}_e| = (\underset{\sim}{J}_e \cdot \underset{\sim}{J}_e)^{1/2} \tag{4}$$

Equations 2 and 4 tacitly assume that all components are equally significant in causing discomfort. That is, a radial jerk or acceleration of a certain magnitude would cause the same level of discomfort as would a normal or fore-aft jerk or acceleration of that same magnitude. [A more general mathematical theory in which this assumption is not made is presented elsewhere (10).] The degree of validity of this assumption is a matter for experimentation, and the answer will depend significantly on the amount of lateral restraint incorporated in the seating. The methods developed in the present paper, however, remain valid even though the assumption is not strictly true. Geometric designs will be obtained by limiting the maximum amount of ϕ and ψ, denoted respectively as ϕ_{max} and ψ_{max}, along a curve. Then one simply sets $\phi_{max} = \min(a_f, a_\ell, a_n)$ and $\psi_{max} = \min(J_f, J_\ell, J_n)$, where a_f, a_ℓ, and a_n are acceleration limits in respectively the fore-aft, lateral, and normal modes and J_f, J_ℓ, and J_n are the respective jerk limits in those modes. It may also be remarked that the present treatment excludes discomfort caused by motion about a body axis (e.g., rolling) and by the simultaneous presence of acceleration and jerk.

Experimental work is needed to determine acceptable levels of ϕ_{max} and ψ_{max}. The present work will present solutions based on $\phi_{max} = 8$ ft/sec^2 and $\psi_{max} = 8$ ft/sec^3. These numbers are consistent with reported experimental work (6) but are somewhat higher than the 0.15 g allowable lateral acceleration suggested by AASHO (3). In any case, it is felt that levels this high would be suitable if passengers were seated and had good lateral restraints.

EFFECT OF SUPERELEVATION

Banking of curves to completely eliminate lateral force on the vehicle is well established in highway, railroad, and automotive test track design. We will show that the bank angle corresponding to zero lateral force also minimizes the discomfort indexes defined by Eqs. 2 and 4. Consider the centerline curve of the guideway to lie in the horizontal plane, and let the angle of bank be θ. Let $\underset{\sim}{k}$ be a unit vector in the vertically upward direction and $\underset{\sim}{p}$ a unit vector in the horizontal direction as shown in Figure 1.

From elementary dynamics (11), the acceleration of the center of mass of the vehicle is given by

$$\underset{\sim}{a} = -v^2\kappa\underset{\sim}{p} + \dot{v}\underset{\sim}{f} \tag{5}$$

where $\kappa = 1/R$ is the centerline curvature, R is the radius of curvature, and v is the speed of the vehicle. From Figure 1 and Eq. 1 it follows that

$$\begin{aligned}\underset{\sim}{a}_e &= -g\underset{\sim}{n} + g\underset{\sim}{k} - v^2\kappa\underset{\sim}{p} + \dot{v}\underset{\sim}{f} \\ &= (-g + g\cos\theta + v^2\kappa\sin\theta)\underset{\sim}{n} + (g\sin\theta - v^2\kappa\cos\theta)\underset{\sim}{\ell} + \dot{v}f\end{aligned} \tag{6}$$

and therefore

$$\phi = |\underset{\sim}{a}_e| = \left[2g^2(1 - \cos\theta) + v^4\kappa^2 - 2gv^2\kappa\sin\theta + \dot{v}^2\right]^{1/2} \tag{7}$$

It may be readily verified that ϕ is minimized by the choice

$$\theta = \theta^* = \tan^{-1}\frac{v^2\kappa}{g} \tag{8}$$

By setting $\underset{\sim}{a} = -v^2\kappa\underset{\sim}{p}$ in Figure 1, it also follows that this choice reduces the lateral component of the thrust on the vehicle to zero. Thus, we have shown that a guideway with a bank angle defined by Eq. 8 will result in zero lateral thrust on the vehicle and will also minimize the acceleration discomfort index ϕ.

From Eqs. 3, 4, and 6 it follows that the effective jerk and jerk discomfort index are respectively given by

$$\begin{aligned}\underset{\sim}{J}_e = {} & (-g\dot{\theta}\sin\theta + 2v\dot{v}\kappa\sin\theta + v^2\dot{\kappa}\sin\theta + v^2\kappa\dot{\theta}\cos\theta)\underset{\sim}{n} \\ & + (g\dot{\theta}\cos\theta - 2v\dot{v}\kappa\cos\theta - v^2\dot{\kappa}\cos\theta + v^2\kappa\dot{\theta}\sin\theta)\underset{\sim}{\ell} + \dot{v}\underset{\sim}{f}\end{aligned} \tag{9}$$

and

$$\begin{aligned}\psi = {} & (g^2\dot{\theta}^2 + 4v^2\dot{v}^2\kappa^2 + v^4\dot{\kappa}^2 + v^4\kappa^2\dot{\theta}^2 + \dot{v}^2 \\ & - 4gv\kappa\dot{\theta}\dot{v} - 2gv^2\dot{\kappa}\dot{\theta} + 4v^3\kappa\dot{v}\dot{\kappa})^{1/2}\end{aligned} \tag{10}$$

We note that bank angle θ does not explicitly appear in the expression for ψ. By equating $\frac{d\psi}{d\dot{\theta}}$ to zero, we obtain

$$\dot{\theta} = \frac{2gv\kappa\dot{v} + gv^2\dot{\kappa}}{g^2 + v^4\kappa^2} \tag{11}$$

as a necessary condition for ψ to attain a minimum. It may then be checked that $\dot{\theta}$ as defined by Eq. 11 is precisely the time derivative of θ^* defined by Eq. 8. This means that, if the bank angle is given by Eq. 8 at all points of the centerline curve, then Eq. 11 will be satisfied. Thus we have shown that a guideway bank angle defined by Eq. 8 will minimize the jerk discomfort index ψ.

Thus we conclude that the bank angle defined by Eq. 8 not only reduces the lateral thrust on the vehicle to zero but also minimizes both discomfort indexes that we have defined. [It is possible to obtain this conclusion for the more general case in which the centerline curve is not restricted to horizontal. Furthermore, a more general form of the function than that assumed in Eq. 2 is possible. The results are presented in a separate report (10).] This bank angle will be referred to hereafter as the optimal bank angle. The discomfort along an optimally banked curve may be obtained by substituting from Eqs. 8 and 11 for θ and $\dot{\theta}$ in Eqs. 7 and 10. The corresponding expressions for the effective acceleration and jerk vectors and the discomfort indexes are given as follows:

$$\begin{aligned}\underset{\sim}{a}_e^* &= [(v^4\kappa^2 + g^2)^{1/2} - g]\underset{\sim}{n} + \dot{v}\underset{\sim}{f} \\ \phi^* &= \{[(v^4\kappa^2 + g^2)^{1/2} - g]^2 + \dot{v}^2\}^{1/2} \\ \underset{\sim}{J}_e^* &= (v^4\kappa^2 + g^2)^{-1/2}\,(2v^3\kappa^2\dot{v} + v^4\kappa\dot{\kappa})\underset{\sim}{n} + \dot{v}\underset{\sim}{f} \\ \psi^* &= (v^4\kappa^2 + g^2)^{-1/2}\,[(2v^3\kappa^2\dot{v} + v^4\kappa\dot{\kappa})^2 + \dot{v}^2(v^4\kappa^2 + g^2)]^{1/2}\end{aligned}$$

In practice, the bank angle could be limited by other considerations, and the value obtained from Eq. 8 would be too high to be practical.

FOUR-SPIRAL SWITCH

The first example we consider is that of a four-spiral curve that can be used as either a merge or diverge switch at stations and interchanges in PRT networks. The four-spiral switch is shown in Figure 2. The equation for the spiral curve is

$$\beta = cs^2 \tag{12}$$

If β is small, then Eq. 12 may be approximated by

$$y = \frac{c}{3} x^3 \tag{13}$$

The spiral set shown in Figure 2 uses four spirals of the form of Eq. 13. The spirals are matched for position, slope, and curvature at junction points 2, 3, and 4. The first spiral winds, the second unwinds, the third winds, and the fourth unwinds. The curvature at points 1, 3, and 5 is zero. Maximum curvature is attained at points 2 and 4. The slope of the spiral set is zero at both ends. The use of the spiral set as a switch permits acceleration and deceleration lanes to be packaged parallel and near to the main traffic lane. It can be shown (1, 12) that

$$c = \frac{16h}{L^3} \tag{14}$$

where h and L are as shown in Figure 2. It follows further from Eqs. 13 and 14 that

$$\kappa \simeq \frac{d^2y}{dx^2} = \frac{32hx}{L^3} \tag{15}$$

We next consider the banking of the switch. It will be assumed that the bank angle varies linearly along each of the four spirals; is zero at points 1, 3, and 5; and attains its maximum value θ_o at the points 2 and 4. It follows immediately that between points 1 and 2 θ is given by the equation

$$\theta = \frac{4\theta_o x}{L} \tag{16}$$

Furthermore, if a vehicle is traveling at speed v, then

$$\dot{\theta} = \frac{4v\theta_o}{L} \tag{17}$$

We next consider the problem of finding the discomfort experienced by traveling at constant speed along the switch. By symmetry it suffices to study the problem only in the first sprial, between 1 and 2. By using Eqs. 13 through 17, it follows that Eqs. 7 and 10 become

$$\phi = \left\{2g^2\left[1 - \cos\left(\frac{4\theta_o x}{L}\right)\right] + 1{,}024\,\frac{h^2v^4x^2}{L^6} - 64ghv^2\,\frac{x}{L^3}\sin\left(\frac{4\theta_o}{L}x\right)\right\}^{1/2}$$

$$\psi = \left(16g^2\theta_o^2\,\frac{v^2}{L^2} + 1{,}024\,\frac{h^2v^6}{L^6} + 16{,}384h^2\theta_o^2 v^6\,\frac{x^2}{L^8} - 256gh\theta_o\,\frac{v^4}{L^4}\right)^{1/2} \tag{18}$$

If on the other hand the four-spiral curve is optimally banked, the bank angle as given by Eq. 8 is

$$\theta^* = \tan^{-1}\left(\frac{32hv^2x}{gL^3}\right) \tag{19}$$

and the discomfort indexes given earlier take the form

$$\phi^* = g\left(1 + 1{,}024\,\frac{h^2v^4x^2}{g^2L^6}\right)^{1/2} - g$$

$$\psi^* = 1{,}024\,\frac{h^2v^5x}{gL^6}\left(1 + 1{,}024\,\frac{h^2v^4x^2}{g^2L^6}\right)^{-1/2} \tag{20}$$

Equations 18 and 20 were programmed on a digital computer to permit numerical investigation. In all computations, h = 8 ft and v = 60 ft/sec were chosen. For selected values of L and θ_o, ϕ and ψ were computed over the range $0 \le x \le L/4$. In every case, both ϕ and ψ attained their maximum values, denoted respectively as ϕ_{max} and ψ_{max}, at $x = L/4$. Figure 3 shows the dependence of ϕ_{max} and ψ_{max} on the switch length. The curves show that a substantial reduction of discomfort can result from banking.

It is of interest to graphically depict the switch length reduction possible with banking as shown in Figure 4. The figure is a design curve based on the design assumptions of $\phi_{max} \le 8$ ft/sec^2 and $\psi_{max} \le 8$ ft/sec^3. The curve was obtained by solving Eq. 18 by trial and error with $x = L/4$. The procedure was to fix θ_o and vary L by small increments over a wide range. The value of L corresponding to $\psi_{max} = 8$ ft/sec^3 was then found. In every case, ϕ_{max} was less than ψ_{max}. By doing this for several values of θ_o, we obtained the data shown in Figure 4. Values of θ_o in the range $0 \le \theta_o \le \theta^*$ were selected. It follows by setting $x = L/4$ in Eq. 19 that $\theta^* = 3/8$ radian (21 deg 30 min).

RIGHT ANGLE TURN

A right angle turn may be accomplished by means of a circular arc blended with the straight at both ends through spiral curves as shown in Figure 5. We shall design the right angle turn with no banking to keep $\psi \le 8$ ft/sec^2 and then investigate the effect that banking has in reducing discomfort. Vehicle speed in the right angle turn will be taken as constant.

Because the angle β_o over which the spiral extends need not be small, we discard the approximation introduced in Eq. 13 and use Eq. 12 exactly for the spiral curve. From Eq. 12 we have

$$\kappa = \frac{d\beta}{ds} = 2cs = 2c^{1/2}\beta^{1/2}$$

$$\dot{\kappa} = 2cv, \quad \dot{\beta} = 2csv = 2c^{1/2}v\beta^{1/2} \tag{21}$$

Furthermore, if the bank angle θ varies linearly along the spiral, it follows that

$$\theta = \kappa s = \kappa c^{-1/2}\beta^{1/2}$$

If the maximum bank angle is θ_o, then

$$\theta_o = \kappa c^{-1/2}\beta_o^{1/2} \tag{22}$$

and thus, substituting for κ,

$$\theta = \theta_o(\beta/\beta_o)^{1/2} \tag{23}$$

Substituting from Eqs. 21 and 22 in Eqs. 7 and 10 gives the following discomfort indexes:

$$\phi = [2g^2(1 - \cos\theta) + 4cv^4\beta - 4gc^{1/2}v^2\beta^{1/2}\sin\theta]^{1/2}$$

$$\psi = \left(g^2c\theta_o^2\frac{v^2}{\beta_o} + 4c^2v^6 + 4c^2v^6\theta_o^2\frac{\beta}{\beta_o} - 4gc^{3/2}\theta_o\frac{v^4}{\beta_o^{1/2}}\right)^{1/2} \tag{24}$$

In particular, for the unbanked curve putting $\theta_o = 0$, we have

$$\phi = 2c^{1/2}v^2\beta^{1/2}$$

$$\psi = 2cv^3 \tag{25}$$

If the maximum allowable values for ϕ and ψ are ϕ_o and ψ_o respectively, we have

$$c = \frac{\psi_o}{2v^3}$$

$$\beta_o = \frac{\phi_o^2}{2\psi_o v} \tag{26}$$

Furthermore, because the curvatures are to be matched at the point where the spiral and circular curves blend and the curvature of the spiral at this point is $\kappa_o = 2c^{1/2}\beta_o^{1/2}$, we obtain the radius of the circular arc R as

$$R = \frac{1}{\kappa} = \frac{1}{2\sqrt{c\beta_o}} = \frac{v^2}{\phi_o} \tag{27}$$

Equations 26 and 27 completely determine the geometry of the right angle turn. To get an idea of the space taken up by the curve, we define two terms L_c and D as shown in Figure 5. The distance D is of importance when how the interchange fits in with existing road patterns and structures is considered. For the spiral we have

$$\frac{dx}{ds} = \cos\beta \qquad \frac{dy}{ds} = \sin\beta$$

Using Eq. 12 and integrating these equations approximately with the help of Taylor series expansions for cos β and sin β, we get

$$x = c^{-1/2}\left(\beta^{1/2} - \frac{1}{5}\beta^{5/2}\right)$$

$$y = c^{-1/2}\left(\frac{1}{3}\beta^{3/2} - \frac{1}{21}\beta^{7/2}\right) \tag{28}$$

If (x_o, y_o) are the coordinates of the point P where the spiral and circular arcs blend, a little geometric analysis shows that

$$L_c = x_o + y_o + 2R\sin(\pi/4 - \beta_o)\cos\pi/4$$

$$D = y_o \sec\pi/4 + R\sin(\pi/4 - \beta_o) - R[1 - \cos(\pi/4 - \beta_o)]$$

Substituting from Eq. 28 gives

$$L_c = c^{-1/2}\left(\beta_o^{1/2} + \frac{1}{3}\beta_o^{3/2} - \frac{1}{5}\beta_o^{5/2} - \frac{1}{21}\beta_o^{7/2}\right) + \sqrt{2}\,R\sin(\pi/4 - \beta_o)$$

$$D = \sqrt{2}\,c^{-1/2}\left(\frac{1}{3}\beta_o^{3/2} - \frac{1}{21}\beta_o^{7/2}\right) + R[\sin(\pi/4 - \beta_o) - 1 + \cos(\pi/4 - \beta_o)] \tag{29}$$

The parameters for the unbanked right angle turn obtained from Eqs. 26, 27, and 29 are summed up as follows:

$$\beta_o = \tfrac{1}{4} \text{ rad} = 14 \text{ deg } 20 \text{ min} \qquad L_c = 40.2 \text{ ft}$$

$$R = 32 \text{ ft} \qquad D = 13.7 \text{ ft}$$

(variable values: $v = 16$ ft/sec, $\phi_o = 8$ ft/sec^2, $\psi_o = 8$ ft/sec^3)

To investigate the effect of banking this curve on discomfort, we programmed Eq. 24 on a digital computer, and the values of ϕ and ψ were obtained for several values of θ_o, the maximum bank angle. Numerical values were found at several points along the curve. In every case, the discomfort indexes attained their maximum value at the point P. The maximum value of each discomfort index for motion along the curve at a constant speed of 16 ft/sec is plotted against the bank angle in Figure 6, which brings out the considerable reduction in discomfort possible by introducing banking.

GRADE CHANGE

To analyze a grade change, we first analyze discomfort along a curve with zero superelevation in the vertical plane. If the tangent to the curve is inclined at γ to the horizontal, the acceleration components for motion along such a curve are

$$\underset{\sim}{a}_e = -g\underset{\sim}{n} - \underset{\sim}{g} + \underset{\sim}{a} = -g\underset{\sim}{n} - (g \sin\gamma \underset{\sim}{f} - g \cos\gamma \underset{\sim}{n}) + (-v^2\kappa\underset{\sim}{n} + \dot{v}\underset{\sim}{f}) \tag{30}$$

We consider two possible methods of traversing a curve in the vertical plane, namely, constant speed ($\dot{v} = 0$) and zero thrust. In the latter case, vehicle acceleration is solely due to gravity and $\dot{v} = g \sin\gamma$. The expressions thus obtained for the effective acceleration and jerk and the discomfort indexes are presented as follows, where the subscript c denotes constant speed motion and subscript z denotes zero thrust motion.

$$(\underset{\sim}{a}_e)_c = [-g(1 - \cos\gamma) - v^2\kappa]\underset{\sim}{n} - g \sin\gamma \underset{\sim}{f}$$

$$\phi_c = [2g^2(1 - \cos\gamma) + v^4\kappa^2 + 2gv^2\kappa(1 - \cos\gamma)]^{1/2}$$

$$(\underset{\sim}{J}_e)_c = (-g\dot{\gamma} \sin\gamma - v^2\dot{\kappa})\underset{\sim}{n} - g\dot{\gamma}\cos\gamma \underset{\sim}{f}$$

$$\psi_c = (g^2\dot{\gamma}^2 + v^4\dot{\kappa}^2 + 2gv^2\dot{\gamma}\dot{\kappa} \sin\gamma)^{1/2}$$

$$(\underset{\sim}{a}_e)_z = [-g(1 - \cos\gamma) - v^2\kappa]\underset{\sim}{n}$$

$$\phi_z = g(1 - \cos\gamma) + v^2\kappa$$

$$(\underset{\sim}{J}_e)_z = (-g\dot{\gamma} \sin\gamma - v^2\dot{\kappa} - 2gv\kappa \sin\gamma)\underset{\sim}{n}$$

$$\psi_z = |-g\dot{\gamma} \sin\gamma - v^2\dot{\kappa} - 2gv\kappa \sin\gamma|$$

A grade change may be accomplished by means of a straight sloping line connected to the horizontal at either end by two spirals as shown in Figure 7. If the straight segment is eliminated, the grade change just becomes a vertical version of the four-spiral curve of Figure 2. Such a curve was used as a grade change for an automotive test track (1). We will compare the discomfort in traversing the grade change for the zero thrust and constant speed cases.

In the zero thrust motion, maximum speed is attained at point 5 and maximum discomfort is attained in the lower half of the grade change. For the constant speed case the discomforts in the lower and upper halves are equivalent. Therefore we consider only the bottom two spiral curves in Figure 7. Taking the origin at point 5 as shown in Figure 7 and matching slope and curvature at points 3 and 4 yields the following equations for two spirals:

Figure 1. Banked guideway and acceleration.

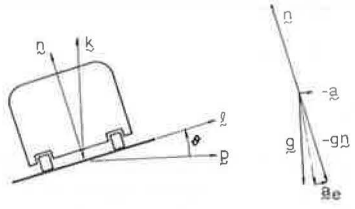

Figure 2. Four-spiral switch.

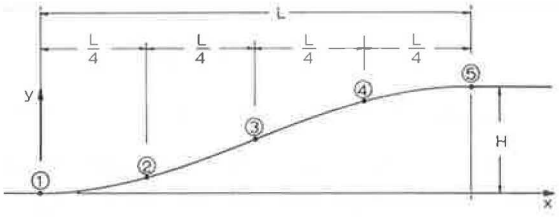

Figure 3. Discomfort indexes versus switch length.

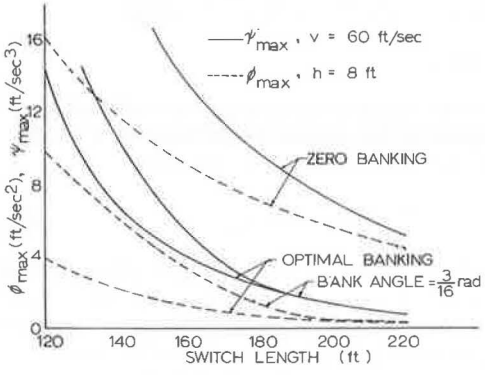

Figure 4. Switch length versus bank angle.

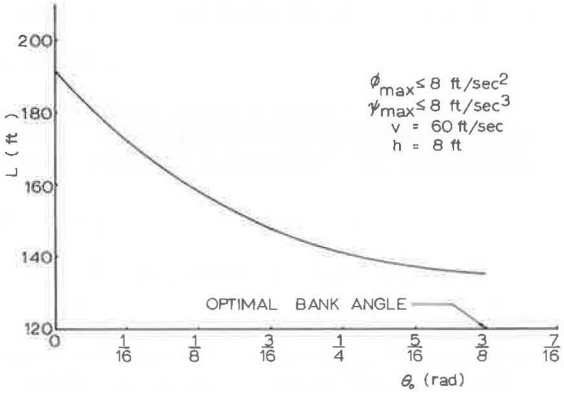

Figure 5. Right angle turn.

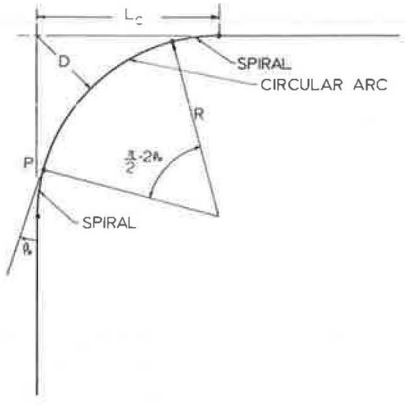

Figure 6. Discomfort in a right angle turn.

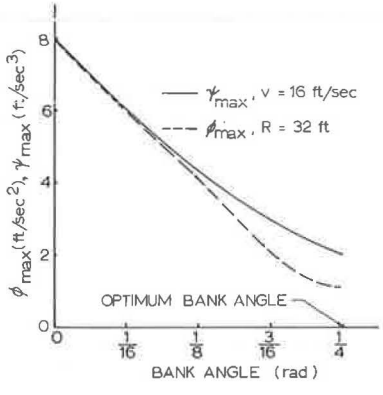

$$\beta = \frac{2\alpha}{L'^2} x^2 \quad 0 \leq x \leq L'/2$$

$$\beta = -\frac{2\alpha}{L'^2} x^2 + \frac{4\alpha}{L'} x - \alpha \quad L'/2 < x \leq L' \tag{31}$$

where, because of the small angles involved, we have replaced s by x.

By substituting these expressions for β in the formulas for effective acceleration and jerk and discomfort indexes, we obtain the expressions for ϕ_z, ψ_z, ϕ_o, ψ_o, and the discomfort indexes for zero thrust and constant speed motions for each of the two bottom spiral curves of the grade change. The expressions are given in the Appendix and were programmed on a digital computer to find the discomfort indexes at several points from 3 to 5. Because the speed along the grade change varies in the zero thrust case, the speed for constant speed motion may be taken equal to either the maximum speed or the minimum speed of the zero thrust case. For numerical computations the following values were chosen:

$$\begin{aligned} H &= \text{level difference} = 10 \text{ ft} \\ v &= \text{minimum speed} = 16 \text{ ft/sec} \\ \alpha &= \text{maximum slope} = 0.20 \text{ radian (11 deg 27 min)} \end{aligned} \tag{32}$$

The corresponding maximum speed for zero thrust motion turns out to be 29.93 ft/sec. The maximum values of the discomfort indexes were found for zero thrust motion and for motion at constant speeds of 16 ft/sec and 29.93 ft/sec and are shown in Figure 8. It is observed that the discomfort for constant speed motion at the higher speed is considerably more than for zero thrust motion.

McConnell (1) considered only the centripetal component of the acceleration $v^2\kappa$ and the corresponding jerk in evaluating discomfort. Denoting the corresponding discomfort indexes by ϕ_M and ψ_M we have

$$\phi_M = v^2\kappa$$

$$\psi_M = |v^2\dot{\kappa}| \tag{33}$$

The expressions obtained on substituting for κ and $\dot{\kappa}$ in Eq. 33 are also included in the Appendix. It is of interest to investigate the degree of error introduced by this assumption. To do this, we compared the maximum discomfort as given by Eq. 33 with the values obtained for $(\phi_o)_{max}$ and $(\psi_o)_{max}$ from the expressions in the Appendix. This was done for two values of the speed, v = 16 ft/sec and v = 60 ft/sec, and two values of the maximum inclination, α = 0.20 radian (11 deg 27 min) and α = 0.40 radian (2 deg 17 min). The results are given in Table 1.

The effect of the speed is readily observable. A study of the expressions given earlier indicates that at higher speeds the centripetal component provides the major contribution to ϕ_o and ψ_o and therefore ϕ_M and ψ_M provide better approximations to ϕ_o and ψ_o at higher speeds than at lower speeds. As for the effect of inclination at a given speed, the expressions indicate that, as the inclination increases, the approximate expressions (Eq. 33) would become less accurate. However, for any realistic angle of grade, the inclinations would still be fairly small, and therefore the error in Eq. 33 is not very sensitive to variations of the inclination. These conclusions are borne out by the numerical values given in Table 1.

ACKNOWLEDGMENT

This work was supported in part by the Urban Mass Transportation Administration, U.S. Department of Transportation.

Figure 7. Grade change.

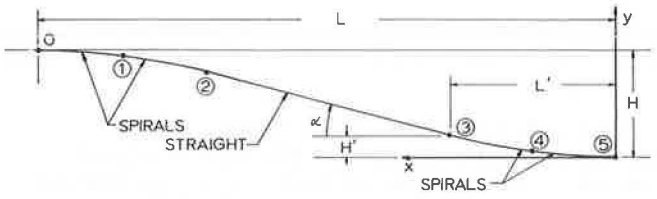

Figure 8. Discomfort on a grade change.

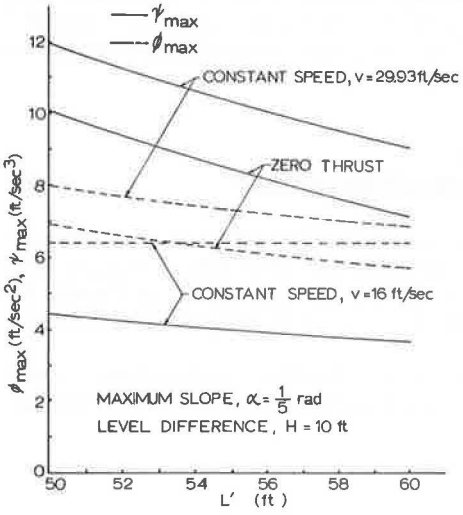

Table 1. Contribution of fore-aft component to discomfort.

Maximum Slope (rad)	Speed (ft/sec)	$(\varphi_o)_{max}$ (ft/sec²)	$(\varphi_m)_{max}$ (ft/sec²)	$(\psi_c)_{max}$ (ft/sec³)	$(\psi_m)_{max}$ (ft/sec³)
$\alpha = 0.20$	v = 16	6.39	0.68	1.39	0.15
	v = 60	10.27	9.60	9.65	7.68
$\alpha = 0.04$	v = 16	1.28	0.14	0.28	0.03
	v = 60	2.03	1.92	1.86	1.54

Note: L' = 150 ft.

REFERENCES

1. McConnell, W. A. Human Sensitivity to Motion as a Criterion for Highway Curves. HRB Bull. 149, 1957.
2. Stonex, K. A. Automotive Test Track Design. HRB Bull. 149, 1957.
3. A Policy on Geometric Design of Rural Highways. AASHO, 1965.
4. Length of Railway Transition Spiral Analysis and Running Tests. Association of American Railroads, Rept. ER-37, 1963.
5. Fraser, T. M. Human Response to Sustained Acceleration. NASA Rept., 1966.
6. Cabtrack Studies. Royal Aircraft Establishment, Rept. 68287, Pt. 1, Dec. 1968 and Pt. 2, Jan. 1969.
7. Anderson, J. W. An Exploratory Study of Combined Forces on Horizontal Transitions to Sharp Curves. Yale Univ., thesis for certificate in highway transportation, 1966.
8. Hamilton, W. F., II, and Nance, D. K. Systems Analysis of Urban Transportation. Scientific American, July 1969.
9. Sobey, A. J., and Cone, J. W. The Case for Personal Rapid Transit. Highway Research Record 367, 1971.
10. Dais, J. L., and Balachandra, M. Motion Discomfort and Transportation Guideway Form. To be published.
11. Goodman, L. E., and Warner, W. H. Dynamics. Wadsworth, 1963.
12. Dais, J. L. Minichanges, Stations and Geometry in PRT. In Personal Rapid Transit—A Collection of Papers on a New Type of Urban Transportation (Anderson, J. E., Dais, J. L., Garrard, W. L., and Kornhauser, A. L., eds.), Univ. of Minnesota Extension Division, March 1972.

APPENDIX

DISCOMFORT EXPRESSIONS FOR FOUR-SPIRAL GRADE CHANGE

Spiral 1: $0 < x < L'/2$

$$\beta = \frac{2\alpha}{L'^2} x^2 \qquad \kappa = \frac{4\alpha}{L'^2} x \qquad \dot{\kappa} = \frac{4\alpha}{L'^2} v$$

$$\phi_z = g(1 - \cos\beta) + \frac{4\alpha}{L'^2} v^2 x$$

$$\psi_z = 12 \frac{g\alpha}{L'^2} vx \sin\beta + \frac{4\alpha}{L'^2} v^3$$

$$\phi_o = \left[2g^2(1 - \cos\beta) + \frac{16\alpha^2}{L'^4} v^4 x^2 + \frac{8g\alpha}{L'^2} v^2 x (1 - \cos\beta)\right]^{1/2}$$

$$\psi_o = \frac{4\alpha v}{L'^2} (g^2 x^2 + v^4 + 2gv^2 x \sin\beta)^{1/2}$$

$$\phi_M = \frac{4\alpha}{L'^2} v^2 x$$

$$\psi_M = \frac{4\alpha}{L'^2} v^3$$

Spiral 2: $L'/2 < x < L'$

$$\beta = -\frac{2\alpha}{L'^2} x^2 + \frac{4\alpha}{L'} x - \alpha \qquad \kappa = \frac{4\alpha}{L'} \left(1 - \frac{x}{L'}\right) \qquad \dot{\kappa} = -\frac{4\alpha v}{L'^2}$$

$$\phi_z = g(1 - \cos\beta) + \frac{4\alpha}{L'} v^2 \left(1 - \frac{x}{L'}\right)$$

$$\psi_z = \left| - \frac{12g\alpha}{L'} v \left(1 - \frac{x}{L'}\right) \sin\beta + \frac{4\alpha}{L'^2} v^3 \right|$$

$$\phi_o = \left[2g^2(1 - \cos\beta) + \frac{16\alpha^2}{L'^2} v^4 \left(1 - \frac{x}{L'}\right)^2 + \frac{8g\alpha}{L'} v^2 \left(1 - \frac{x}{L'}\right)(1 - \cos\beta) \right]^{1/2}$$

$$\psi_o = \frac{4\alpha v}{L'} \left[g^2 \left(1 - \frac{x}{L'}\right)^2 + \frac{v^4}{L'^2} - \frac{2gv^2}{L'} \left(1 - \frac{x}{L'}\right) \sin\beta \right]^{1/2}$$

$$\phi_M = \frac{4\alpha}{L'} v^2 \left(1 - \frac{x}{L'}\right)$$

$$\psi_M = \frac{4\alpha}{L'^2} v^3$$